Photoredox Catalysis for the Fabrication of Water-Repellent Surfaces with Application for Oil/Water Separation

Yelan Xiao,[1,2] Shun-Cheung Cheng,[1] Yongyi Feng,[1] Zhen Shi,[3] Zhenjia Huang,[4] Gary Tsui,[4] Clement Manohar Arava,[5] Vellaisamy A. L. Roy[6] and Chi-Chiu Ko[1]*

[1]Department of Chemistry and State Key Laboratory in Marine Pollution, City University of Hong Kong, Tat Chee Avenue, Kowloon Tong, Hong Kong 999077, China

[2]School of Science and Engineering, The Chinese University of Hong Kong (Shenzhen), Shenzhen 518172, China

[3]Institute of Advanced Magnetic Materials, College of Materials and Environmental Engineering, Hangzhou Dianzi University, Hangzhou 310012, People Republic of China

[4]Department of Industrial and Systems Engineering, The Hong Kong Polytechnic University, Hung Hom, Kowloon, Hong Kong 999077, China

[5]Department of Materials Science & Engineering, City University of Hong Kong, Kowloon Tong, Hong Kong 999077, China

[6]James Watt School of Engineering, University of Glasgow, Glasgow G128QQ, United Kingdom

KEYWORDS: water-repellent, hydrophobicity, oleophilicity, photoredox catalysis, surface modification, oil/water separation

ABSTRACT: Silanization processes with perfluoroalkyl silanes have been demonstrated to be effective in developing advanced materials with many functional properties, including hydrophobicity, water repellency and self-cleaning properties. However, practical industrial applications of perfluoroalkyl silanes are limited by their extremely high cost. On the basis of our recent work on photoredox catalysis for amidation with perfluoroalkyl iodides, its application for surface chemical modification on filter paper, as an illustrative example, has been developed and evaluated. Before photocatalytic amidation, the surface is functionalized with amine functional groups by silanization with 3-(trimethoxysilyl)propylamine. All chemically-modified surfaces have been fully characterized by ATR-IR, XPS, SEM-EDS, and 3D profiler to confirm the successful silanization and photocatalytic amidation. After surface modification of the filter papers with perfluoroalkanamide, they show high water repellency and hydrophobicity with contact angles over 120°. These filter papers possess high wetting selectivity, which can be used to effectively separate the organic and aqueous biphasic mixtures. The perfluoroalkanamide-modified filter papers can be used for separating organic/aqueous biphasic mixtures over many cycles without lowering the separating efficiency, indicating its reusability and excellent durability.

INTRODUCTION

Surface chemical modifications for developing advanced materials with novel functional properties have been one of the most popular research fields over recent decades because these materials have found applications in many different areas.[1-5] Amongst various functional groups used in surface modifications, fluorinated hydrocarbons, which possess unique wettability arisen from their hydrophobicity, have attracted particular attention. Surface modifications with fluorinated hydrocarbons have wide-ranging applications such as self-cleaning,[6-8] antifogging,[9]

anti-icing,[10-12] anti-corrosion,[13-15] stain resistance,[16,17] drag reduction,[18,19] microfluidic devices,[20] atmospheric water capture,[21] water-oil separation,[22-29] biomaterials,[30,31] and smart windows,[32] etc.

On the other hand, the studies of the interfacial science of natural lotus leaves and water striders have shown that low surface energy materials can be produced by functionalizing hydrophobic molecular moieties on the surface with hierarchical roughness.[33,34] This has become the fundamental design for advanced materials with low surface energy.[35] Based on this fundamental understanding, various techniques, such as plasma deposition,[36] physical or chemical vapor deposition,[37,38] atomic layer deposition,[39] micro- or nano-particle deposition,[40-43] and the sol-gel method[44] and the photochemical method,[45] have been developed to modify the surface morphologies and introduce the superhydrophobic features of advanced materials. Despite many successful demonstrations of the above methodologies, practical applications of most of these approaches are limited as they are costly, complicated, time-consuming, or unsuitable with an industrial scale-up processes.

Silanization processes with fluoroalkyl substituted silanes have been demonstrated to be useful for surface modification and the development of materials with advanced coatings.[46-51] However, the practical industrial applications of fluoroalkyl-substituted silanes in silanization processes are very limited due to its low reaction efficiencies in the silanization, the instability of these silanes for recovery/reuse, and the very high cost of fluoroalkyl-substituted silanes. With our recent work on photocatalytic fluoroalkylation using low-cost and readily accessible perfluoroalkyl iodides,[52-54] their successful applications for surface chemical functionalization would significantly reduce the cost of surface modification with fluoroalkyl functional moieties. Besides, photochemical surface modification together with a photomask enables the fabrication of patterned surfaces,

which have many important applications.[55- 62] Although the photocatalytic processes for surface modification with organofluorine compounds have not been reported, the feasibility of photocatalytic reactions for successful surface functionalization has been demonstrated. In this work, surface functionalization by photocatalytic amidation with perfluoroalkyl iodides (Scheme 1) have been evaluated. Photocatalytic amidation is chosen because surface functionalization with amine group by silanization with low-cost 3-(trimethoxysilyl)propylamine (APTMS) has been well-documented. Moreover, the wettability, hydrophobicity and applications of the materials with their surfaces chemically modified by this method will be studied. With this strategy for surface functionalization, it is foreseeable that it could also be applied to any surfaces with hydroxyl groups, including glass, paper, wood, natural fibers and textile materials, which could have significant impacts in both academia and industry.

Scheme 1. Photocatalytic amidation of (a) APTMS and (b) APTMS-functionalized surface with perfluorooctyl iodide.

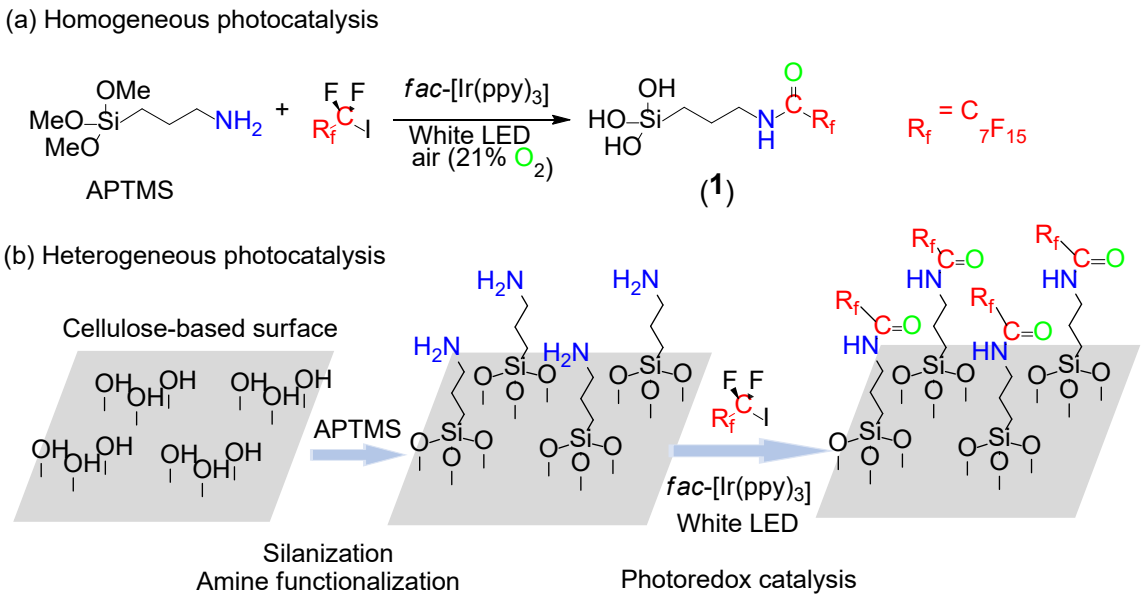

RESULTS AND DISCUSSION

Photoredox Catalysis of Perfluorooctyl Iodide with Aminoalkylsilane

To evaluate the applicability of our recently reported photocatalytic amidation[52,53] for surface functionalization, the reaction between trimethoxylsilyl substituted amine (APTMS) and perfluorooctyl iodide ($C_8F_{17}I$) (Scheme 1a) was studied. The reaction gave the product of *N*-[3-(trihydroxylsilyl)propyl] perfluorooctanamide (**1**), indicating the hydrolysis of the methoxy groups during the photocatalytic reaction. The product was purified by column chromatography with silica gel and characterized by IR, ^{1}H NMR, ^{19}F NMR, ^{13}C{^{1}H} NMR spectroscopy, mass spectrometry and elemental analysis. The isolated yield of 20.5%, which is much lower than reactions for other substituted amines,[52,53] can be attributed to the silanization of the glassware and silica gel used in the reaction and purification. The purified product **1** shows a strong characteristic ν(C=O) at 1691 cm^{-1} in the IR spectrum (Figure 1), similar to the related amide analogs reported in our previous research work.[52,53] The *N*-[3-(trihydroxysilyl)propyl] group can be characterized by ^{1}H NMR spectroscopy (Figure S2); whereas the perfluorooctamide moiety can be characterized by ^{19}F NMR spectroscopy (Figure S3). With ^{13}C{^{1}H} NMR spectroscopy (Figure S4), the C signals of both *N*-[3-(trihydroxylsily)propyl] and perfluorooctamide groups as well as the C=O in the peptide linkage, have been characterized. The linkage between *N*-[3-(trihydroxysilyl)propyl] and perfluorooctamide groups has also been further confirmed by mass spectrometry and element analysis (Supporting Information).

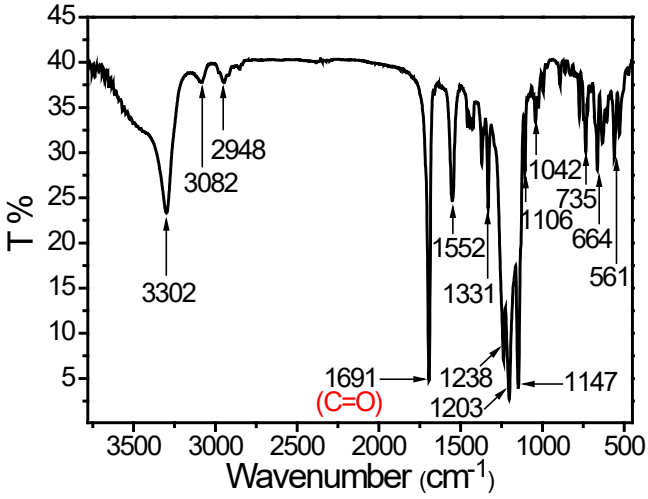

Figure 1. FT-IR spectrum of **1** in KBr disc.

Photocatalytic Amidation for Surface Functionalization of Cellulose-Based Surface

As the photocatalytic amidation works well with silyl functional groups, it is anticipated that this photoredox reaction could also be applicable for surface functionalization on solid supports with silanized amine functional group. To evaluate this application, filter paper as an illustrative example of cellulose-based solid-support materials with hydroxyl functional groups on their surfaces has been used. The surface of filter paper was first chemically modified with APTMS to introduce the amine groups prior to functionalization by photocatalytic amidation with perfluoroalkyl iodide (Scheme 1b).

As shown in Scheme 1b, the filter paper surface was initially modified with $-NH_2$ groups by treatment with APTMS according to a modified literature procedure (See Supporting Information).[63] Optimization of the amine-functionalization has been performed with different concentrations of APTMS solutions. The efficiency of amine functionalization has been evaluated by the increase of weight, Si and N elemental compositions determined by SEM-EDS, and the

surface roughness detected by Zygo 3D optical profiler of the APTMS-modified filter papers (Table 1, Figures S5-S9). In general, the weight as well as the Si and N elemental compositions of the APTMS-modified filter paper increase with the concentration of APTMS solution (Table 1). This suggests the increase of APTMS surface modification with a higher concentration of APTMS solution. From the change of N compositions against the APTMS concentration, the percentage of amine functionalization reaches a plateau when 0.84 M of APTMS is used. Comparing the pristine filter paper, the surface roughness of the amine-functionalized surfaces increases from ~ 0.50 μm to ~ 0.70 μm after APTMS modification (Table 1).

Table 1. Physical and surface characteristics of APTMS-modified filter papers **S1**–**S5**.[a]

Filter Paper	APTMS solution[b]	Increased weight (g)	Si content (%)	N content (%)	Increased roughness (μm)
S1	1	0.00357	4.86	4.18	0.498±0.033
S2	2	0.00425	5.95	4.96	0.667±0.018
S3	3	0.00683	6.53	5.58	0.661±0.038
S4	4	0.01074	7.82	6.03	0.685±0.035
S5	5	0.01121	8.26	6.13	0.694±0.027

[a]The data were calculated based on the average values of 12 pieces of filter papers. The filter papers were cut into small pieces (2 cm × 2 cm) for this experiment. [b]For APTMS solutions 1–5: APTMS (150 mg, 750 mg, 1.50 g, 2.25 g and 3.00 g for solutions 1–5, respectively) dissolved in a 15-mL ethanol/water (v/v: 4/1) mixture.

After surface modification with APTMS, the filter papers exhibit some degree of water repellency. This property is revealed from the wettability test, based on the contact angle (CA) measurements with a water droplet on APTMS-modified filter papers over different times after deposition (Figure 2). As shown in Figures 2a and 2b, the APTMS-modified filter papers **S1** and **S2** show water an initial CA of *ca.* 70–73°, but the water droplets would be readily absorbed by the filter papers within several seconds. Filter paper **S3** shows a similar property as **S1** and **S2** but

with a much slower absorption rate as indicated by the decrease of the CA from initially 82.8° to 74.2° after 1 min of deposition. After 10 minutes of deposition, the water droplet would be completely absorbed (Figure 2c). This shows that both the contact angle and water repellency increase with the degree of APTMS modification. Further increase of the water repellency and contact angle is observed in the filter papers **S4** and **S5** (Figures 2d and 2e). For these filter papers, the initial contact angles are about 100° and would only decrease to about 80° after 10-min of deposition, indicating the slow absorption rate. Although the silane-content increases from **S4** to **S5**, the water contact angles of these filter paper are similar. This is likely attributed to the polymerization and aggregation of APTMS at high concentration, which result in different surface properties.[64] These results show that the APTMS concentration used for **S4** is optimal for amine functionalization of the filter paper with the highest water repellency. With APTMS-modified filter paper **S4**, its surface was further functionalized by photocatalytic amidation with perfluorooctyl iodide using *fac*-[Ir(ppy)$_3$] as photocatalyst (Scheme 1b).

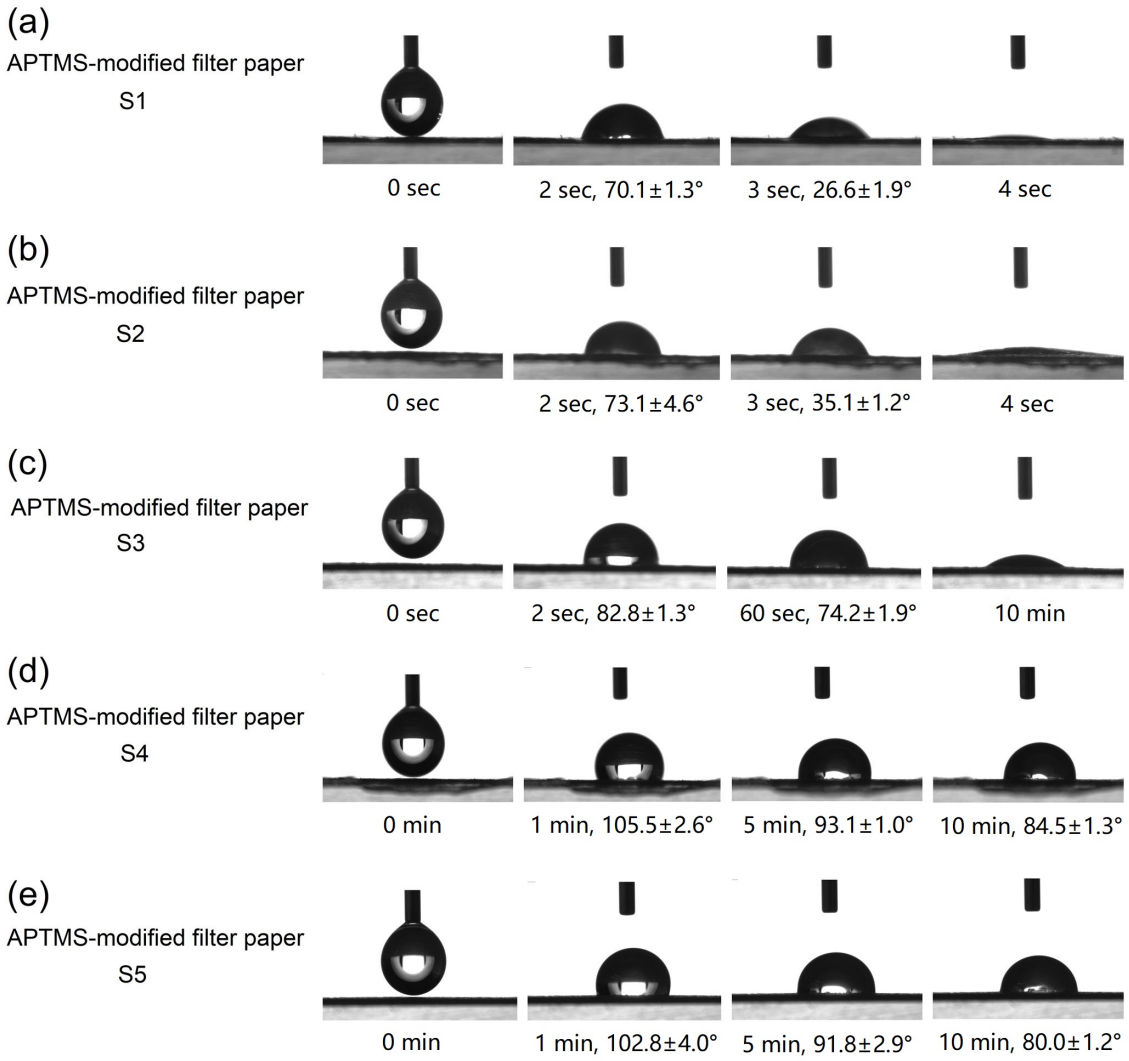

Figure 2. Contact angle measurements on APTMS-modified filter papers **S1** – **S5** at different times after deposition of the water droplet.

The chemically-modified surfaces were characterized by ATR-IR spectroscopy (Figure 3b). Since there is a significant overlapping of the IR absorption bands in the regions 900 – 1500 cm^{-1} and 2800 – 3500 cm^{-1} in pristine and chemically modified filter papers, the analysis of the variation of the IR absorption in these regions associated with the chemical modifications is difficult, even though notable changes of the absorption intensity for certain bands, such as 1202 and 1242 cm^{-1} can be observed. The evolution of the new band at 1556 cm^{-1} in APTMS-treated filter paper, which

is a characteristic absorption of APTMS and absent in untreated filter paper, confirmed the successful silanization of filter paper by APTMS. After photocatalytic amidation of the APTMS-modified filter paper with perfluorooctyl iodide after 60-minute photoirradiation, a new absorption shoulder at 1684 cm^{-1}, attributable to the ν(C=O) of the amide group (Figure 3) was observed. Related amide ν(C=O) of perfluorooctanamide is observed at 1691 cm^{-1} (Figure 1). Moreover, there is significant enhancement of the absorption intensities of bands at 1242 and 1202 cm^{-1}, which correspond to two strong characteristic absorption bands observed in the IR spectrum of perfluorooctanamide (Figure 3a). These IR absorption features substantiate the successful application of photocatalysis for the amide functionalization on the APTMS-modified filter paper with perfluorooctyl iodide.

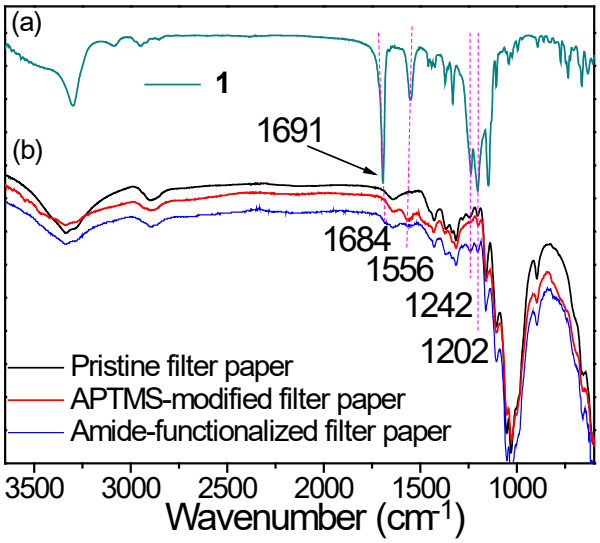

Figure 3. (a) FTIR spectrum of **1** and (b) overlaid FTIR spectra of pristine filter paper, APTMS-modified filter paper before and after photocatalytic amidation (60-minutes irradiation) recorded on an ATR mode.

The chemical compositions of the pristine, APTMS-modified and perfluorooctanamide-functionalized filter paper were further examined by X-ray photoelectron spectroscopy (XPS). In the XPS spectrum of the pristine filter paper (Figure S10), it only shows peaks corresponding to C and O signals. Upon treatment with APTMS, signals of Si and N are characterized (Figure S11). This indicates the successful chemical modification of APTMS onto the filter paper. For perfluorooctanamide-functionalized filter paper, in addition to the expected C 1s (282 – 294 eV) and O 1s (528 – 535 eV) signals, signals corresponding to Si 2p (100 – 104 eV), N 1s (396 – 403 eV) and F 1s (682 – 691 eV) are also observed in the survey XPS spectrum, which suggest the successful chemical modifications. Deconvolution analysis of the high resolution signals of C 1s, Si 2p, N 1s, O 1s and F 1s shows the existence peaks of C-Si (283.86 eV), C-C (285.16 eV), C=O (287.21 eV), C-O (290.85 eV), C-F (293.24 eV); Si-C (101.59 eV), Si-O (102.01 eV); NH-C (398.98 eV); N-C=O (400.95 eV); O-Si (530.06 eV); O=C (531.37 eV); O-C or H-O-C (531.38 eV); F-C (688.17 eV); and inorganic fluoride (684.03 eV), respectively. These bonds provide another form of evidence confirming the successful silanization and photocatalytic amide formation in surface modifications.

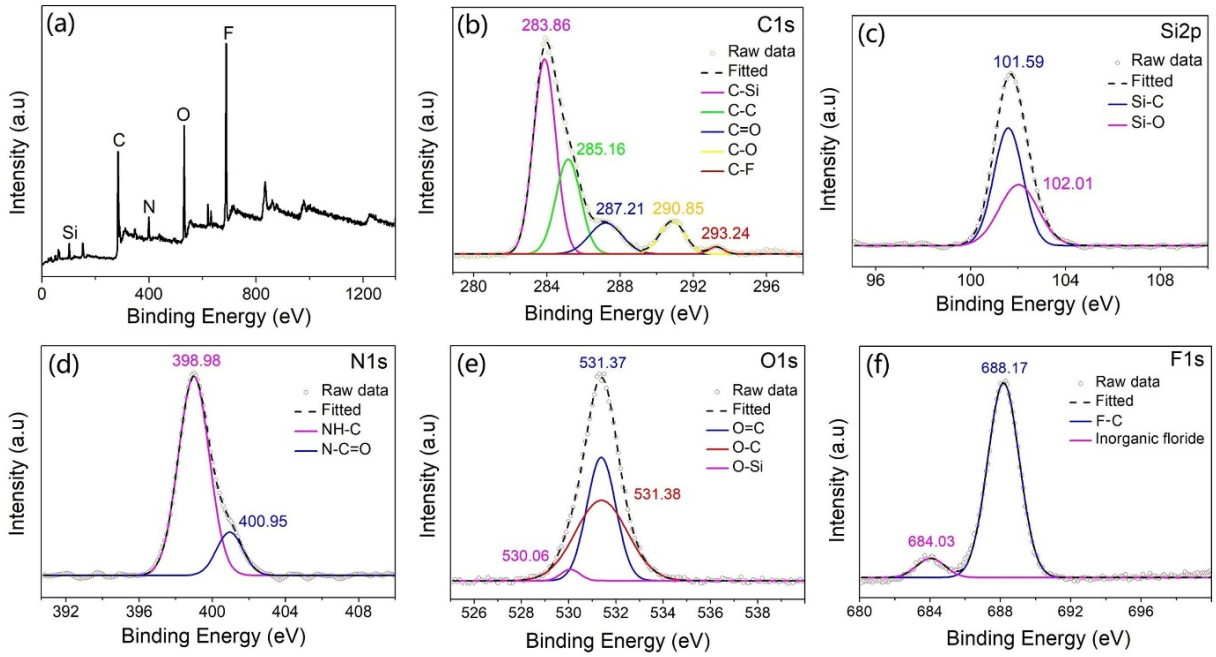

Figure 4. (a) XPS survey spectrum of the perfluorooctanamide-functionalized filter paper and deconvoluted fittings of the high resolution (b) C 1s, (c) Si 2p, (d) N 1s, (e) O 1s and (f) F 1s signals.

The surface characteristics of the filter papers before and after chemical modifications have also been studied using SEM, EDS and 3D optical profiler (Figure 5). The surface morphologies of pristine (Figure 5a), APTMS-modified (**S4**, Figure 5b), and perfluorooctanamide-functionalized (Figure 5c) filter papers are shown in the SEM images. These images reveal the high micro- and nanoscale surface roughness of the cellulose fibers on their surfaces. The differences in surface roughness and morphologies (Figure 5a2, b2, and c2) are supportive of successful chemical modifications by treatment of APTMS and photocatalytic amidation. The presence of elements silicon (Si) (7.82 wt.%) and nitrogen (N) (6.03 wt.%) in APTMS-modified filter paper (Figure 5e) as well as Si (6.98 wt. %), N (5.63 wt.%) and fluorine (F) (6.73 wt.%) in perfluorooctanamide-functionalized filter paper (Figure 5f) further corroborate the successful surface modifications. The

distributions of different elements in perfluorooctanamide-functionalized filter paper based on scanning electron microscopy with energy-dispersive spectroscopy (SEM-EDS) mapping (Figure 6) confirm the widespread functionalization of the fibers with APTMS and perfluorooctanamide.

It is worth noting that more connections are present at the interfaces between cellulose fibers upon silanization with APTMS. This is likely due to the bridging ability of the silane anchoring groups. As a result, the microscale surface roughness increases (6.72 μm *vs.* 6.04 μm before treatment) with considerably different surface morphology as revealed in 3D optical profiler topography images (Figure 5h *vs.* Figure 5g). As further functionalization of amine groups on the APTMS-modified filter paper with the perfluorooctanamide functional moiety would only affect the surface on a nanoscale level, the overall roughness and surface morphology are not significantly altered, as revealed in Figure 5h and 5i.

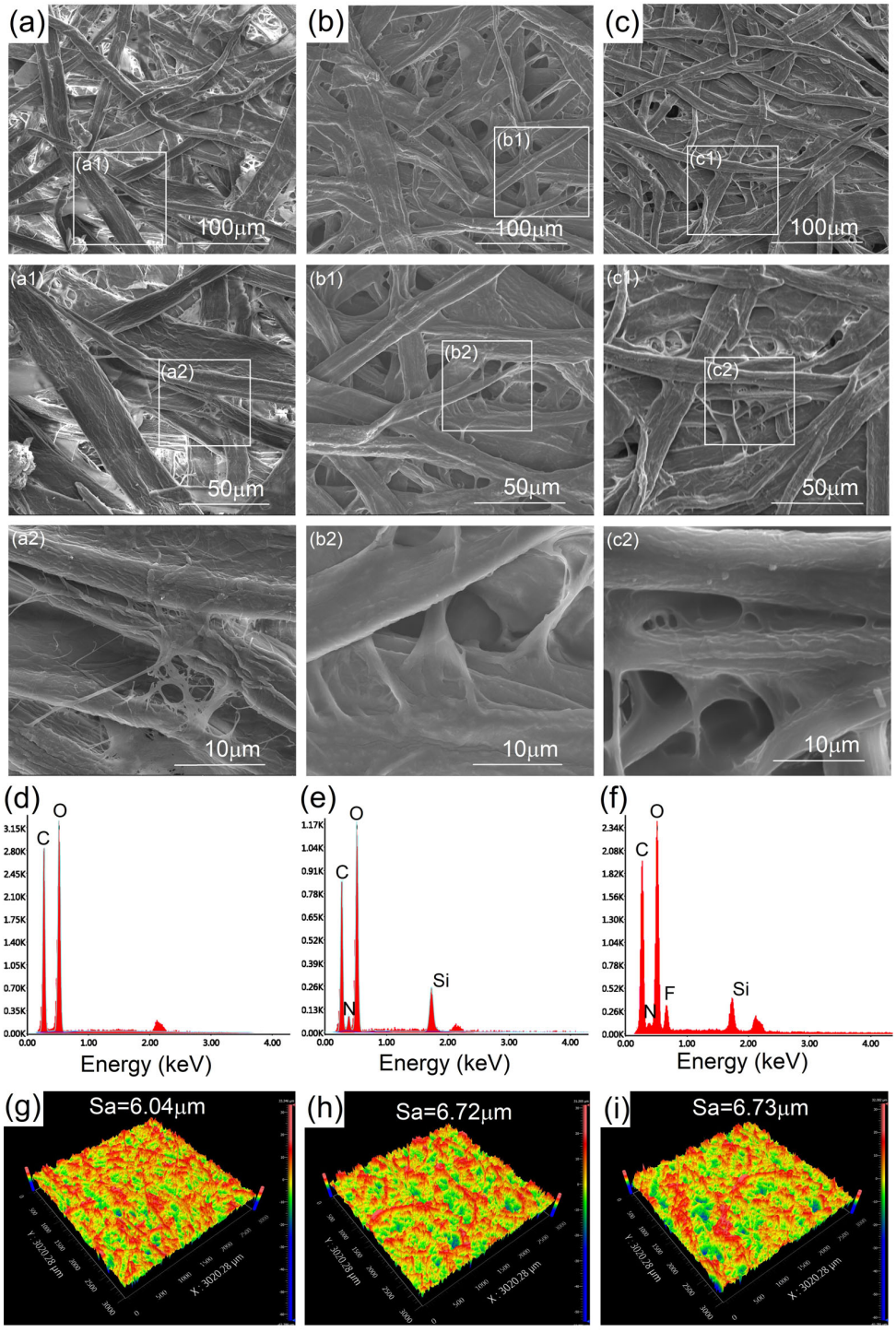

Figure 5. SEM images (a-c), EDS analysis (d-f) and 3D optical profiler topography images (g-i) of (a, d, g) pristine filter paper, (b, e, h) APTMS-modified filter paper (**S4**) and (c, f, i) perfluorooctanamide-functionalized filter paper.

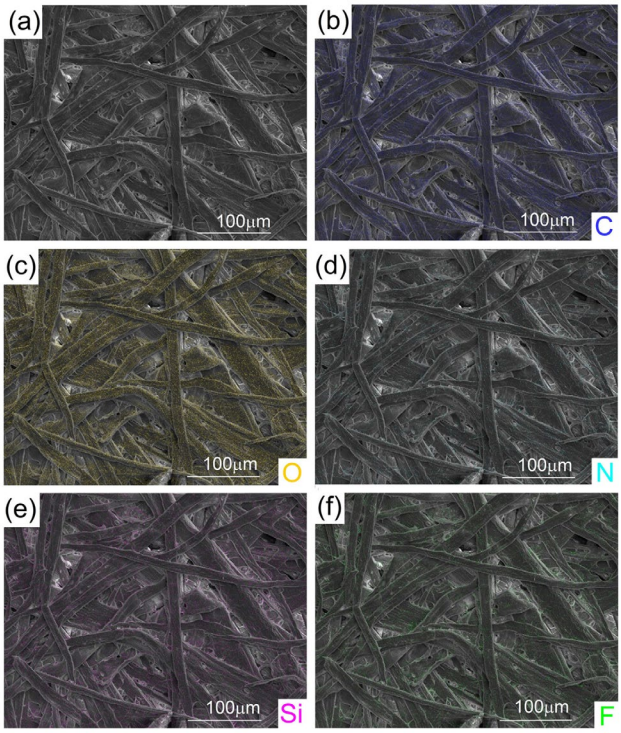

Figure 6. (a) SEM image and SEM-EDS mapping of (b) C, (c) O, (d) N, (e) Si and (f) F on the surface of the perfluorooctanamide-functionalized filter paper.

Wettability of the Chemically-Modified Cellulose-Based Filter Paper

The filter paper exhibits excellent water repellency and hydrophobicity after surface functionalization through chemical modifications with APTMS and perfluorooctanamide. This property was studied using wettability tests based on the contact angle measurements with a water droplet (Figure 7). As revealed in Figures 7a-c, water droplet is readily absorbed by pristine filter paper, and thus the CA is 0°; whereas the droplets can rest on the APTMS-modified and perfluorooctanamide-functionalized filter papers with initial CAs of 105.5° and 126.0°, respectively. This indicates the hydrophilic cellulose surface becomes hydrophobic after chemical modification with APTMS and perfluorooctanamide. The increase of CA from 105.5° to 126.0° after the functionalization of the perfluorooctanamide group is consistent with the increased

hydrophobicity and lower surface energy of the perfluoroalkyl group. However, superhydrophobicity with contact angle ≥ 150° cannot be achieved as the roughness of the micro/nano structure of the perfluorooctanamide-functionalized filter paper are not typical range for superhydrophoic surface.[65]

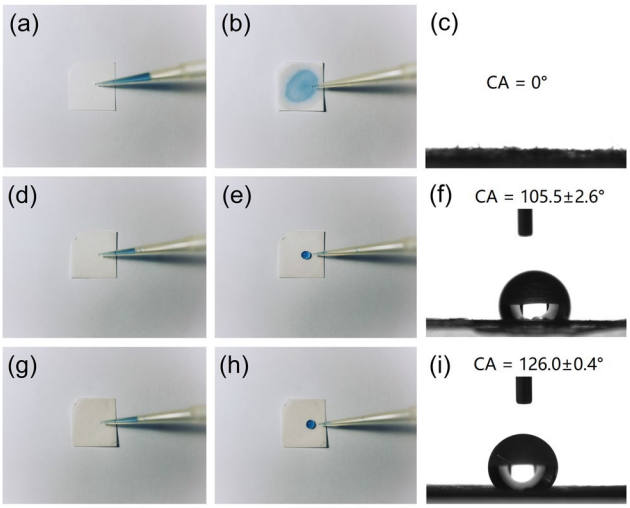

Figure 7. Photographs showing the wettability tests on filter papers and contact angle measurements: (a), (b) and (c) pristine filter paper; (d), (e) and (f) APTMS-modified filter paper; (g), (h) and (i) perfluorooctanamide-functionalized filter paper.

To determine water repellency in a semi-quantitative manner, contact angle measurements of water droplets on APTMS-modified (Figure 2d) and perfluorooctanamide-functionalized (Figure 8) filter papers at different times after deposition have been performed. For APTMS-modified filter paper (**S4**), the CA initially after deposition reaches approximately 105° but it decreases to 93° and 84° upon standing for 5 and 10 minutes, respectively (Figure 2d). The considerable decrease of CA upon standing for 10 minutes is ascribed to the absorption of water as reflected from the noticeable decreased volume of the water droplet. In contrast, the CA of the water droplets on

perfluorooctanamide-functionalized filter papers only slightly decreases after standing on the filter papers for 5 and 10 minutes (Figure 8). This observation indicates a significant increase in the water repellency of the filter paper upon conversion of the amide group to perfluorooctanamide. Comparing perfluorooctanamide-functionalized filter papers prepared from different irradiation times (30-minutes, 60-minutes, and 120-minutes irradiation), a slight increase of initial CAs with irradiation time but with a similar extent of change in CAs upon standing are noted (Figures 8a, 8b and 8c). This suggests that these perfluorooctanamide-functionalized filter papers have similar hydrophobicity and water repellency.

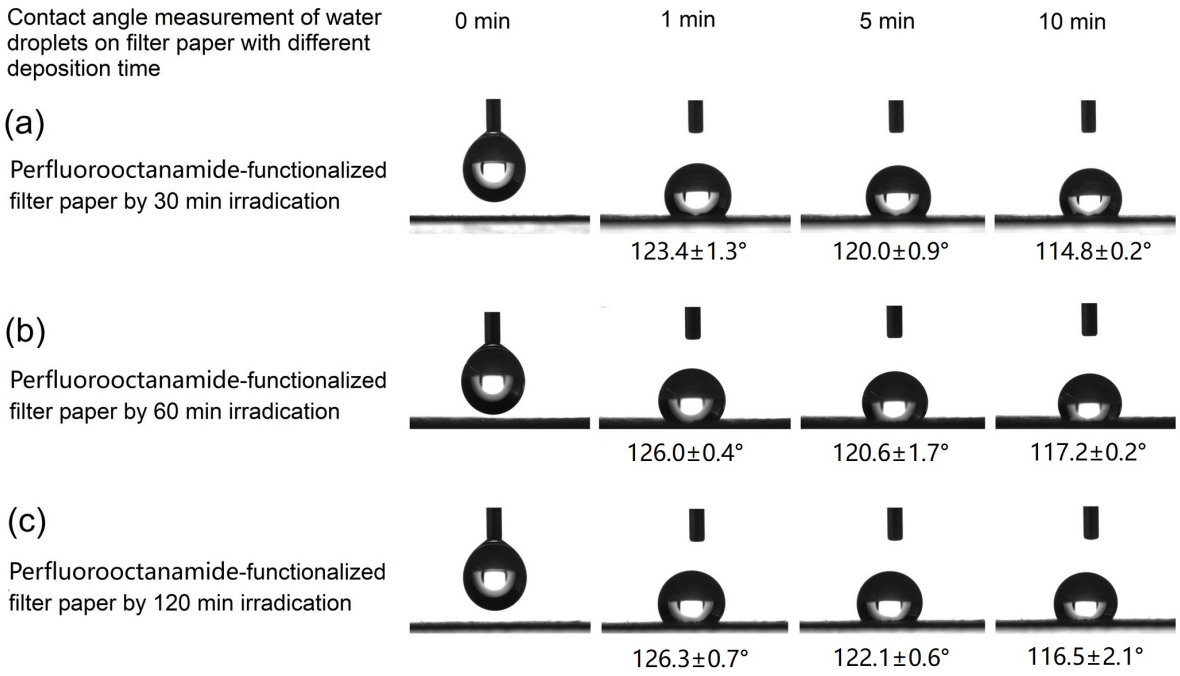

Figure 8. Contact angles measurements on filter papers with surface functionalization by photocatalytic amidation with perfluorooctyl iodide upon irradiation for (a) 30, (b) 60, and (c) 120 mins.

In view of the high water-repellency and hydrophobicity of the perfluorooctanamide-modified filter papers, these surfaces might possess wetting selectivity between hydrophobic organic

solvents and water. Such selectivity would enable these materials for applications in separating oil/water mixtures.[22-29,66- 71] To investigate the wetting selectivity of the perfluorooctanamide-functionalized filter paper for hydrophobic organic solvents and water, it is initially assessed by studying the penetrating properties of the filter paper with an *n*-hexane/water mixture, which is prepared by adding a hexane droplet (20 μL) onto the blue-dyed water droplet (20 μL) rested on the perfluorooctanamide-modified filter paper (Figure 9). As discussed above, the water droplet would not be absorbed by the filter paper and remains stable resting on the filter paper. In contrast, the *n*-hexane droplet would be absorbed and penetrated through the perfluorooctanamide-functionalized filter paper (Figures 9c and 9d). This indicates the hydrophobicity and oleophilicity of the modified surface. Similarly, droplets of other organic solvents such as *n*-pentane, chloroform, toluene, dichloromethane, petroleum ether and peanut oil would penetrate into this perfluorooctanamide-functionalized filter paper immediately after deposition.

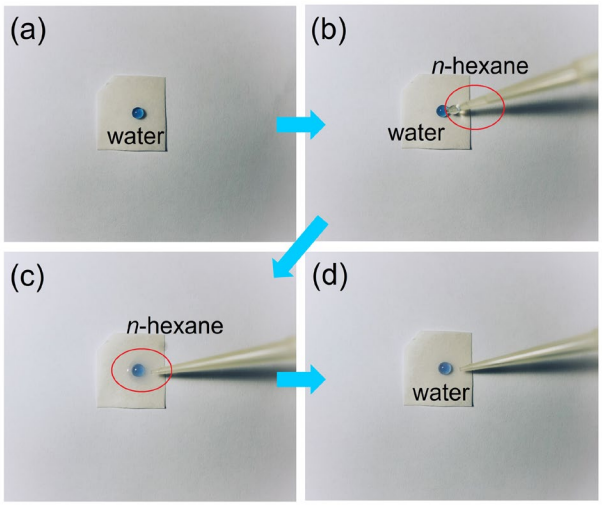

Figure 9. The preliminary wetting selectivity assessment of perfluorooctanamide-functionalized filter paper with *n*-hexane/water mixture, prepared by adding a *n*-hexane droplet (20 μL) onto the blue-dyed water droplet (20 μL) rested on the filter paper.

To study the applications of this surface-modified filter paper for aqueous-organic biphasic separation, perfluorooctanamide-functionalized filter paper with a diameter of 9 cm (Figure 10a) was prepared by treatment of APTMS similar to that for **S4** and then functionalization by photocatalytic amidation with perfluorooctyl iodide upon 60-min irradiation. To evaluate the aqueous-organic biphasic separation efficiency, different organic solvent/water mixtures (10 mL, v/v, 1:1) have been used to test the separation by pouring into a filter funnel fitted with a quadrant-folded perfluorooctanamide-functionalized filter paper. The solvent capable of penetrating through the filter paper was collected by the conical flask in the bottom. As demonstrated in the separation of n-hexane/water mixture (Figure 10b), only organic solvents could penetrate through the filter paper and be collected in the collecting flask, whereas the aqueous layer with blue-color dye remained resting on the filter paper. The collected organic solvents showed no observable mixing with water (Figure 10b; Videos in Supporting Information). After removal of the blue-dyed aqueous layer, the filter paper did not show any blue color. This suggested that no aqueous solution can penetrate through the filter paper in the separation processes. In contrast, both *n*-hexane and water can be pass through the pristine filter paper and collected in the collecting flask in a similar control experiment with pristine filter paper (Figure 10c; Videos in Supporting Information). The penetration and absorption of water in the pristine filter paper is also confirmed by the blue dye adsorbed on the filter paper. After ten separation cycles of *n*-hexane/water, the filter paper maintained its high separation efficiency (> 92%), and the average separation efficiency is about 95% (**Figure 10d**) with the average separation flux of 1765 L m^{-2} h^{-1}. After ten cycles of oil/water separation, no obvious change of the chemical composition nor morphology in the filter paper is noted from the ATR-IR (Figure S12) and SEM (Figure S13) characterization. Apart from the *n*-hexane/water mixture, the separation efficiencies using the same filter paper for different solvent

mixtures, including *n*-pentane/water, dichloromethane/water, chloroform/water, toluene/water, petroleum ether/water, ethyl acetate/water, and peanut oil/water, have also determined based on five separation cycles (**Figure 10e**). Except for the peanut oil/water mixture, the separations of all these mixtures can be completed within 6 min with the averaged separation efficiencies larger than 92%. The loss of the solvent or peanut oil by the filter paper due to absorption and evaporation during the separation are summarized in Table S2. Due to the high viscosity of peanut oil, it took about two hours for complete separation with a lower separation efficiency of 81%. The above organic/water separation tests were all conducted with the same perfluorooctanamide-functionalized filter paper. This confirmed the reusability, durability of the water-repellent properties, and the stability of the perfluorooctanamide-functionalized filter paper. However, the filter paper is unable to separate organic solvents from emulsifier-free hexane-in-water (oil-in-water) and octanol-water-ethanol (water-in-oil) emulsions.

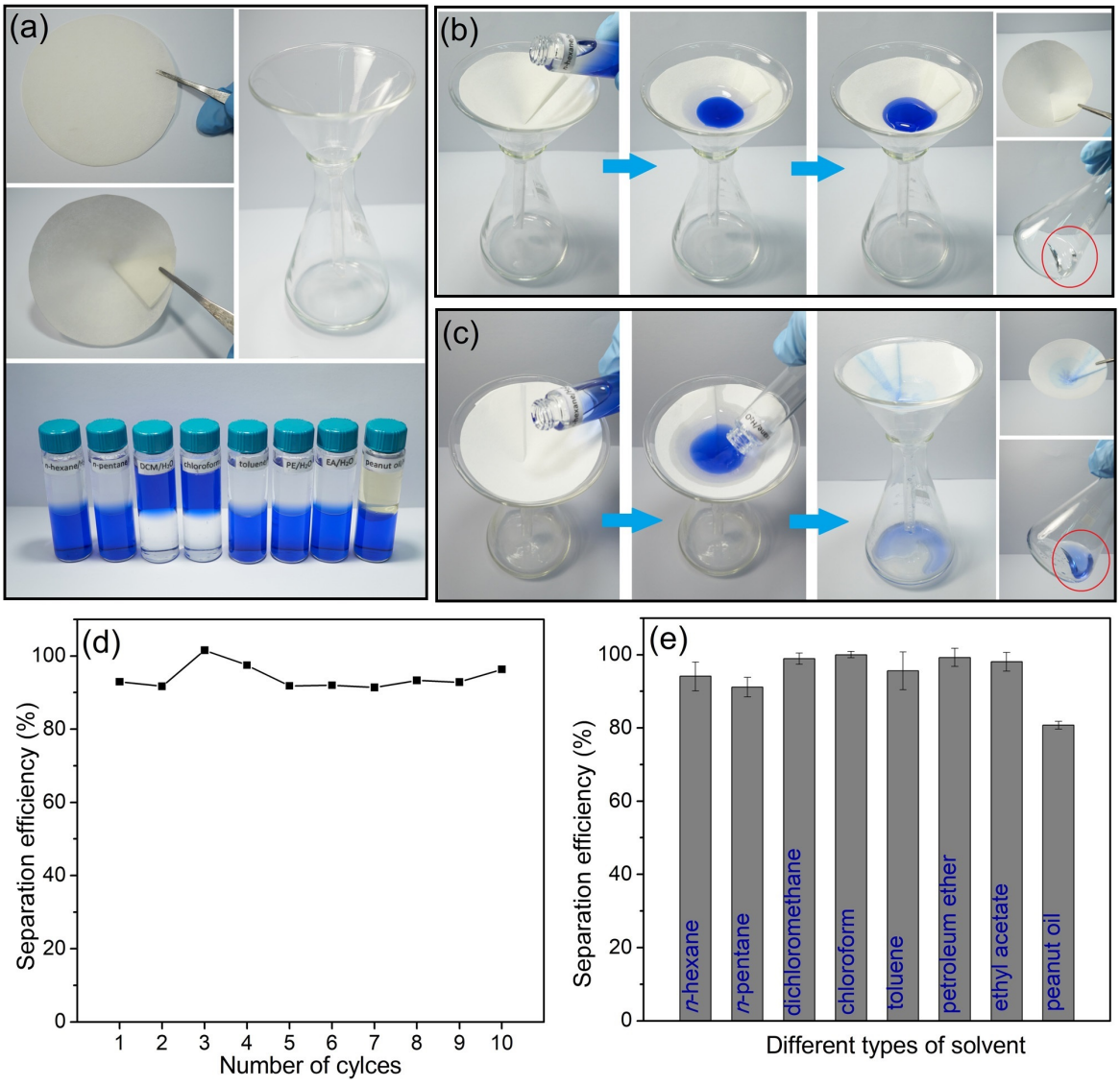

Figure 10. (a) Photographs of the filtration setup with perfluorooctanamide-functionalized filter paper and the organic solvent/water mixtures (10 mL; v/v,1:1) for testing the separating solvent mixtures application. Photographs of *n*-hexane/water mixture separation test with (b) a perfluorooctanamide-functionalized filter paper, and (c) a pristine filter paper. (d) Separation efficiencies of *n*-hexane/water mixture over ten cycles. (e) Separation efficiencies for different organic solvent/water mixtures determined based on five separation cycles with the same filter paper.

CONCLUSIONS

In summary, the photoredox catalysis for the amidation of amines with perfluoroalkyl halides not only tolerate a silane functional moiety under a homogeneous condition but could also work heterogeneously for surface chemical modification. Through two-step processes, silanization with amine functional group and the subsequent photocatalytic amidation with perfluoroalkyl iodide, surface chemical modification with perfluorooctanamide can be achieved with low-cost and readily available amine-containing silanization reagents and perfluoroalkyl iodide. The successful chemical modifications of these surfaces have been characterized by ATR-IR spectroscopy, XPS, SEM-EDS and 3D optical profiler. Further, our results also demonstrate that perfluorooctanamide-functionalized filter papers become hydrophobic with high water repellency, wetting selectivity, and oleophilicity. Importantly, these perfluorooctanamide-functionalized filter papers can be used to effectively separate organic and aqueous biphasic mixtures. With the photochemical method, it is anticipated that patterned surface modification, which can bring additional functional properties, can be achieved using a suitable photomask. The use of this surface functionalization strategy on different materials including fabrics and wood for developing other functional materials is in progress. Our preliminary experiments confirm its applicability for modification of wood and cement surfaces (Figure S14–S16 in Supporting Information).

ASSOCIATED CONTENT

Supporting Information

The Supporting Information is available free of charge on the ACS Publications website at http://pubs.acs.org. General experimental, characterization and copies of ^{1}H, ^{19}F and $^{13}C\{^{1}H\}$

NMR spectra of the amide product from homogenous photocatalysis, detailed synthesis procedures for homogenous and heterogenous photocatalysis reactions (PDF); and videos showing the organic-aqueous biphasic separation using perfluorooctanamide-functionalized filter paper.

AUTHOR INFORMATION

Corresponding Author

*E-mail: vinccko@cityu.edu.hk. Phone: (+852)-3442-6958. Fax: (+852)-3442-0522.

Notes

The authors declare no competing financial interest.

ACKNOWLEDGMENT

This work has been supported by General Research Fund (Project Nos. CityU 11306819 and CityU 11306820) from the Research Grants Council of the Hong Kong SAR, China. Yelan Xiao acknowledges receipt of a University Postgraduate Studentship administrated by City University of Hong Kong. The Advanced Coatings Applied Research Laboratory from Department of Mechanical and Biomedical Engineering of City University of Hong Kong is acknowledged for contact angle measurement. The State Key Laboratory of Ultra-Precision Machining Technology of The Hong Kong Polytechnic University is acknowledged for surface roughness characterization using 3D optical profiler and contact angle measurement.

REFERENCES

(1) Anton, D. Surface-Fluorinated Coatings. *Adv. Mater.* **1998**, *10*, 1197-1205.

(2) Grainger, D. W.; Stewart, C. W. *Fluorinated Surfaces, Coatings, and Films, ACS Symposium Series, Chapter 1: Fluorinated Coatings and Films: Motivation and Significance,* American Chemical Society: Washington DC, 2001.

(3) Liu, T.; Kim, C. J. Turning A Surface Superrepellent even to Completely Wetting Liquids. *Science* **2014**, *346*, 1096-1100

(4) Griffini, G.; Bella, F.; Nisic, F.; Dragonetti, C.; Roberto, D.; Levi, M.; Bongiovanni, R.; Turri, S. Multifunctional Luminescent Down-Shifting Fluoropolymer Coatings: A Straightforward Strategy to Improve the UV-Light Harvesting Ability and Long-Term Outdoor Stability of Organic Dye-Sensitized Solar Cells. *Adv. Energy Mater.* **2015**, *5*, 1401312.

(5) Liu, J.; Sun, Y.; Zhou, X.; Li, X.; Kappl, M.; Steffen, W.; Butt, H.-J. One-Step Synthesis of a Durable and Liquid-Repellent Poly(dimethylsiloxane) Coating. *Adv. Mater.* **2021**, *33*, 2100237.

(6) Fürstner, R.; Barthlott, W. Wetting and Self-Cleaning Properties of Artificial Superhydrophobic Surfaces. *Langmuir* **2005**, *21*, 956-961.

(7) Zhang, X.; Li, Z.; Liu, K.; Jiang, L. Bioinspired Multifunctional Foam with Self-Cleaning and Oil/Water Separation. *Adv. Funct. Mater.* **2013**, *23*, 2881-2886.

(8) Fu, Y.; Jiang, J.; Zhang, Q.; Zhan, X.; Chen, F. Correction: Robust Liquid-Repellent Coatings Based on Polymer Nanoparticles with Excellent Self-Cleaning and Antibacterial Performances. *J. Mater. Chem. A* **2017**, *5*, 275-284.

(9) Faustini, M.; Nicole, L.; Boissière, C.; Innocenzi, P.; Sanchez, C.; Grosso, D. Hydrophobic, Antireflection, Self-Cleaning, and Antifogging Sol-Gel Coatings: An Example of Multifunctional Nanostructured Materials for Photovoltaic Cells. *Chem. Mater.* **2010**, *22*, 4406-4413.

(10) Cheng, T.; He, R.; Zhang, Q.; Zhan, X.; Chen, F. Magnetic Particle-Based Super-hydrophobic Coatings with Excellent Anti-icing and Thermoresponsive Deicing Performance. *J. Mater. Chem. A* **2015**, *3*, 21637-21646.

(11) Shen, Y.; Wu, Y.; Zhu, C.; Chen, H.; Wu, Z.; Xie, Y. Spraying Fabrication of Durable and Transparent Coatings for Anti-icing Application: Dynamic Water Repellency, Icing Delay, and Ice Adhesion. *ACS Appl. Mater. Interface* **2019**, *11*, 3590-3598.

(12) Tang, Y., Zhang, Q.; Zhan, X.; Chen, F. Superhydrophobic and Anti-icing Properties at Overcooled Temperature of Fluorinated Hybrid Surface Prepared via a Sol-Gel Process. *Soft Matter.* **2015**, *11*, 4540-4550.

(13) Weng, C. -J.; Chang, C. -H.; Peng, C. -W.; Yeh, J. -M.; Hsu, C. -L.; Wei, Y. Advanced Anticorrosive Coatings Prepared from the Mimicked Xanthosoma Sagittifolium-leaf-like Electroactive Epoxy with Synergistic Effects of Superhydrophobicity and Redox Catalytic Capability. *Chem. Mater.* **2011**, *23*, 2075-2083.

(14) Nine, M. J.; Cole, M. A.; Johnson, L.; Tran, D. N. H.; Losic, D. Robust Superhydrophobic Graphene-Based Composite Coatings with Self-Cleaning and Corrosion Barrier Properties. *ACS Appl. Mater. Interfaces* **2015**, *7*, 28482-28493.

(15) Xu, Y.; Li, M.; Liu, M. Corrosion and Fouling Behaviors of Phosphatized Q235 Carbon Steel Coated with Fluorinated Polysiloxane Coating. *Progress in Org. Coatings* **2019**, *134*, 177-188.

(16) Nagappan, S.; Choi, M. -C.; Sung, G.; Park, S. S.; Moorthy, M. S.; Chu, S. -W.; Lee, W. -K.; Ha, C. -S. Highly Transparent, Hydrophobic Fluorinated Polymethylsiloxane/Silica Organic-Inorganic Hybrids for Anti-Stain Coating. *Macromolecular Res.* **2013**, *21*, 669-680.

(17) Wu, X.; Liu, M.; Zhong, X.; Liu, G.; Wyman, I.; Wang, Z.; Wu, Y.; Yang, H.; Wang, J. Smooth Water-Based Antismudge Coatings for Various Substrates. *ACS Sustainable Chem. Eng.* **2017**, *5*, 2605-2613.

(18) Zhou. M.; Li, J.; Wu, C.; Zhou, X.; Cai, L. Fluid Drag Reduction on Superhydrophobic Surfaces Coated with Carbon Nanotube Forests (CNTs). *Soft Matter.* **2011**, *7*, 4391-4396.

(19) Hu, H.; Wen, J.; Bao, L.; Jia, L.; Song, D.; Song, B.; Pan, G.; Scaraggi, M.; Dini, D.; Xue, Q.; Zhou, F. Significant and Stable Drag Reduction with Air Rings Confined by Alternated Superhydrophobic and Hydrophilic Strips. *Sci. Adv.* **2017**, *3*, e1603288.

(20) Li, C.; Boban, M.; Snyder, S. A.; Kobaku, S. P. R.; Kwon, G.; Mehta, G.; Tuteja, A. Paper-Based Surfaces with Extreme Wettabilities for Novel, Open-Channel Microfluidic Devices. *Adv. Funct. Mater.* **2016**, *26*, 6121-6131.

(21) Song, Y.; Liu, Y.; Jiang, H.; Li, S.; Kaya, C.; Stegmaier, T.; Han, Z.; Ren. L. A Bioinspired Structured Graphene Surface with Tunable Wetting and High Wearable Properties for Efficient Fog Collection. *Nanoscale* **2018**, *10*, 16127-16137.

(22) Wang, C.; Yao, T.; Wu, J.; Ma, C.; Fan, C.; Fan, Z.; Wang, Z.; Cheng, Y.; Lin, Q.; Yang, B. Facile Approach in Fabricating Superhydrophobic and Superoleophilic Surface for Water and Oil Mixture Separation. *ACS Appl. Mater. Interface* **2009**, *1*, 2613-2617.

(23) Zhang, J.; Seeger, S. Polyester Materials with Superwetting Silicone Nanofilaments for Oil/Water Separation and Selective Oil Absorption. *Adv. Funct. Mater.* **2011**, *21*, 4699-4704.

(24) Zhang, J.; Seeger, S. Polyester Materials with Superwetting Silicone Nnaofilaments for Oil/Water Separation and Selective Oil Absorption. *Adv. Funct. Mater.* **2011**, *21*, 4699-4704.

(25) Zhou, X.; Zhang, Z.; Xu, X.; Guo, F.; Zhu, X.; Men, X.; Ge, B. Robust and Durable Superhydrophobic Cotton Fabrics for Oil/Water Separation. *ACS Appl. Mater. Interfaces* **2013**, *5*, 7208-7214.

(26) Gupta, R. K.; Dunderdale, G. J.; England, M. W.; Hozumi, A. Oil/Water Separation Techniques: A Review of Recent Progresses and Future Directions. *J. Mater. Chem. A* **2017**, *5*, 16025-16058.

(27) Sun, S.; Zhu, L.; Liu, X.; Wu, L.; Dai, K.; Liu, C.; Shen, C.; Guo, X.; Zheng, G.; Guo, Z. Superhydrophobic Shish-kebab Membrane with Self-Cleaning and Oil/Water Separation Properties. *ACS Sustainable Chem. Eng.* **2018**, *6*, 9866-9875.

(28) Yang, C.; Han, N.; Han, C.; Wang, M.; Zhang, W.; Wang, W.; Zhang, Z.; Li, W.; Zhang, X. Design of a Janus F-TiO_2@PPS Porous Membrane with Asymmetric Wettability for Switchable Oil/Water Separation. *ACS Appl. Mater. Interfaces* **2019**, *11*, 22408-22418.

(29) Lin, X.; Hong, J. Recent Advances in Robust Superwettable Membranes for Oil-Water Separation. *Adv. Mater. Interfaces* **2019**, *6*, 1900126.

(30) Privett, B. J.; Youn, J.; Hong, S. A.; Lee, J.; Han, J.; Shin, J. H.; Schoenfisch, M. H. Antibacterial Fluorinated Silica Colloid Superhydrophobic Surfaces. *Langmuir* **2011**, *27*, 9597-9601.

(31) Ueda, E.; Levkin, P. A. Emerging Applications of Superhydrophilic-Superhydrophobic Micropatterns. *Adv. Mater.* **2013**, *25*, 1234-1247.

(32) Bella, F.; Leftheriotis, G.; Griffini, G.; Syrrokostas, G.; Turri, S.; Grätzel, M.; Gerbaldi, C. A New Design Paradigm for Smart Windows: Photocurable Polymers for Quasi-Solid Photoelectrochromic Devices with Excellent Long-Term Stability under Real Outdoor Operating Conditions. *Adv. Funct. Mater.* **2016**, *26*, 1127-1137.

(33) Sun, T.; Feng, L.; Gao, X.; Jiang, L. Bioinspired Surfaces with Special Wettability. *Acc. Chem. Res.* **2005**, *38*, 644-652.

(34) Wu, Y.; Feng, J.; Gao, H.; Feng, X.; Jiang, L. Superwettability-Based Interfacial Chemical Reactions. *Adv. Mater.* **2019**, *31*, 1800718.

(35) Latte, S. S.; Terashima, C.; Nakata, K.; Fujishima, A. Superhydophobic Surfaces Developed by Mimicking Hierarchical Surface Morphology of Lotus Leaf. *Molecules* **2014**, *19*, 4256-4283.

(36) Hubert, J.; Dufour, T.; Vandencasteele, N.; Reniers, F. Synthesis and Texturization Processes of (Super)-Hydrophobic Fluorinated Surfaces by Atmospheric Plasma. *J. Mater. Res.* **2015**, *30*, 3177-3191.

(37) Soto, D.; Ugur, A.; Farnham, K. K.; Varanasi, K. K. Short-Fluorinated iCVD Coatings for Nonwetting Fabrics. *Adv. Funct. Mater.* **2018**, *28*, 1707355.

(38) Fu.Q.; Tu, K.; Goldhahn, C.; Keplinger, T.; Adobes-Vidal, M.; Sorieul, M.; Burgert, I. Luminescent and Hydrophobic Wood Films as Optical Lighting Materials. *ACS Nano* **2020**, *14*, 13775-13783.

(39) Dichiarante, V.; Espinoza, M. I. M.; Gazzera, L.; Vuckovac, M.; Latikka, M.; Cavallo, G.; Raffaini, G.; Oropesa-Nuñez, R.; Canale, C.; Dante, S.; Marras, S.; Carzino, R.; Prato, M.; Ras, R. H. A.; Metrangolo, P. A Short-Chain Multibranched Perfluoroalkyl Thiol for More Sustainable Hydrophobic Coatings. *ACS Sustainable Chem. Eng.* **2018**, *6*, 9734-9743.

(40) Zhang, G.; Lin, S.; Wyman, I.; Zou, H.; Hu, J.; Liu, G.; Wang, J.; Li, F.; Liu, F.; Hu, M. Robust Superamphiphobic Coatings Based on Silica Particles Bearing Bifunctional Random Copolymers. *ACS Appl. Mater. Interfaces* **2013**, *5*, 13466-13477.

(41) Zhan, X.; Yan, Y.; Zhang, Q.; Chen, F. A Novel Superhydrophobic Hybrid Nanocomposite Material Prepared by Surface-Initiated AGET ATRP and Its Anti-icing Properties. *J. Mater. Chem. A* **2014**, *2*, 9390-9399.

(42) Zhang, H.; Ma, Y.; Tan, J.; Fan, X.; Liu, Y.; Gu, J.; Zhang, B.; Zhang, H.; Zhang, Q. Robust, Self-Healing, Superhydrophobic Coatings Highlighted by A Novel Branched Thiol-ene Fluorinated Siloxane Nanocomposites. *Composites Sci. and Tech.* **2016**, *137*, 78-86.

(43) Gao, J.; Wu, L.; Guo, Z.; Li, J.; Xu, C.; Xue, H. A Hierarchical Carbon Nanotube/SiO2 Nanoparticle Network Induced Superhydrophobic and Conductive Coating for Wearable Strain Sensors with Superior Sensitivity and Ultra-Low Detection Limit. *J. Mater. Chem. C* **2019**, *7*, 4199-4209.

(44) Bouvet-Marchand, A.; Graillot, A.; Abel, M.; Koudia, M.; Boutevin, G.; Loubat, C.; Grosso, D. Distribution of Fluoroalkylsilanes in Hydrophobic Hybrid Sol-Gel Coatings Obtained by Co-Condensation. *J. Mater. Chem. A* **2018**, *6*, 24899-24910.

(45) Pester, C. W.; Poelma, J. E.; Narupai, B.; Patel, S. N.; Su, G. M.; Mater, T. E.; Luo, Y.; Ober, C. K.; Hawker, C. J.; Kramer, E. J. Ambiguous Anti-Fouling Surfaces: Facile Synthesis by Light-Mediated Radical Polymerization. *J. Polymer Sci. Part A: Polymer Chem.* **2016**, *54*, 253-262.

(46) Hoque, E.; DeRose, J. A.; Houriet, R.; Hoffmann, P.; Mathieu, H. J. Stable Perfluorosilane Self-Assembled Monolayers on Copper Oxide Surfaces: Evidence of Siloxy-Copper Bond Formation. *Chem. Mater.* **2007**, *19*, 798-804.

(47) Xu, L.; Karunakaran, R. G.; Guo, J.; Yang, S. Transparent, Superhydrophobic Surfaces from One-Step Spin Coating of Hydrophobic Nanoparticles. *ACS Appl. Mater. Interfaces* **2012**, *4*, 1118-1125.

(48) Xiao, Y.; Huang, W.; Tsui, C. P.; Wang, G.; Tang, C. Y.; Zhong, L. Ultrasonic Atomization Based Fabrication of Bio-Inspired Micro-Nano-Binary Particles for Superhydrophobic Composite Coatings with Lotus/Petal Effect. *Composite Part B: Engineering* **2017**, *121*, 92-98.

(49) Huang, W. F.; Xiao, Y. L.; Huang, Z. J.; Tsui, G. C. P.; Yeung, K. W.; Tang, C. Y.; Liu, Q. Super-Hydrophobic Polyaniline-TiO_2 Hierarchical Nanocomposite as Anticorrosion Coating. *Mater. Letters* **2020**, *258*, 126822.

(50) Pan, S.; Guo, R.; Björnmalm, M.; Richardson, J. J.; Li, L.; Peng, C.; Bertleff-Zieschang, N.; Xu, W.; Jiang, J.; Caruso, F. Coatings Super-Repellent to Ultralow Surface Tension Liquids. *Nature Materials* **2018**, *17*, 1040-1047.

(51) Munief, W. -M.; Heib, F.; Hempel, F.; Lu, X.; Schwartz, M.; Pachauri, V.; Hempelmann, R.; Schmitt, M.; Ingebrandt, S. Silane Deposition via Gas-Phase Evaporation and High-Resolution Surface Characterization of the Ultrathin Siloxane Coatings. *Langmuir* **2018**, *34*, 10217-10229.

(52) Ng, C.-O.; Feng, H.; Cheng, S.-C.; Xiao, Y.; Lo, L. T.-L.; Ko, C.-C. Photoredox Catalysis of Cyclometalated Ir^{III} Complex for the Conversion of Amines to Fluorinated Alkyl Amides. *Asian J. Org. Chem.* **2018**, *7*, 1587-1590.

(53) Xiao, Y.; Chun, Y.-K.; Cheng, S.-C.; Ng, C.-O.; Tse, M.-K.; Lei, N-Y.; Liu, R.; Ko, C.-C.

Photocatalytic Amidation and Esterification with Perfluoroalkyl iodide. *Cat. Sci. Tech.* **2021**, *11*, 556-562.

(54) Xiao, Y.; Chun, Y.-K.; Cheng, S.-C.; Liu, R.; Tse, M.-K.; Ko, C.-C. Visible Light Photocatalytic Cross-Coupling and Addition Reactions of Arylalkynes with Perfluoroalkyl Iodides. *Org. Biomol. Chem.* **2020**, *18*, 8686-8693.

(55) Bouriga, M.; Chehimi, M. M.; Combellas, C.; Decorse, P.; Kanoufi, F.; Deronzier, A.; Pinson, J. Sensitized Photografting of Diazonium Salts by Visible Light. *Chem. Mater.* **2013**, *25*, 90-97.

(56) Fors, B. P.; Poelma, J. E.; Menyo, M. S.; Robb, M. J.; Spokeyny, D. M.; Kramer, J. W.; Waite, J. H.; Hawker, C. J. Fabrication of Unique Chemical Patterns and Concentration Gradients with Visible Light. *J. Am. Chem. Soc.* **2013**, *135*, 14106-14109.

(57) Du. T.; Li, B.; Wang, X.; Yu, B.; Pei, X.; Huck, W. T. S.; Zhou, F. Bio-Inspired Renewable Surface-Initiated Polymerization from Permanently Embedded Initiators. *Angew. Chem. In. Ed.* **2016**, *55*, 4260-4264.

(58) Pester, C. W.; Narupai, B.; Mattson, K. M.; Bothman, D. P.; Klinger, D.; Lee, K. W.; Discekici, E. H.; Hawker, C. J. Engineering Surfaces through Sequential Stop-Flow Photopatterning. *Adv. Mater.* **2016**, *28*, 9292-9300.

(59) Delaittre, G.; Goldmann, A. S.; Mueller, J. O.; Barner-Kowollik, C. Efficient Photochemical Approaches for Spatially Resolved Surface Functionalization. *Angew. Chem. Int. Ed.* **2015**, *54*, 11388-11403.

(60) Bella, F.; Griffini, G.; Correa-Baena, J. -P.; Saracco, G.; Grätzel, M.; Hagfeldt, A.; Turri, S.; Gerbaldi, C. Improving Efficiency and Stability of Perovskite Solar Cells with Photocurable Fluoropolymers. *Science* **2016**, *354*, 203-206.

(61) Zoppe, J. O.; Ataman, N. C.; Mocny, P.; Wang, J.; Moraes, J.; Klok, H. -A. Surface-Initiated Controlled Radical Polymerization: State-of-the-Art, Opportunities, and Challenges in Surface and Interface Engineering with Polymer Brushes. *Chem. Rev.* **2017**, *117*, 1105-1318.

(62) Ueda, E.; Levkin, P. A. Patterned Superhydrophobic Surfaces. In Non-wettable Surfaces: Theory, Preparation, and Applications; RSC: **2017**, pp 182 – 222.

(63) Koga, H.; Kitaoka, T.; Isogai, A. *In situ* Modification of Cellulose Paper with Amino Groups for Catalytic Applications. *J. Mater. Chem.* **2011**, *21*, 9356-9361.

(64) Zhang, F.; Srinivasan, M. P. Self-Assembled Molecular Films of Aminosilanes and Their Immobilization Capacities. *Langmuir* **2004**, 20, 2309-2314.

(65) Li, X.-M; Reinhoudt, D.; Crego-Calama, M. What Do We Need for A Superhydrophobic Surface? A Review on the Recent Progress in the Preparation of Superhydrophobic Surfaces. *Chem. Soc. Rev.* **2007**, *36*, 1350-1368.

(66) Chen, B.; Qiu, J.; Sakai, E.; Kanazawa, N.; Liang, R.; Feng, H. Robust and Superhydrophobic Surface Modification by a “Paint + Adhesive” Method: Applications in Self-Cleaning after Oil contamination and Oil-Water Separation. *ACS Appl. Mater. Interfaces* **2016**, *8*, 17659-17667.

(67) Su, X.; Li, H.; Lai, X.; Zhang, L.; Liang, T.; Feng, Y.; Zeng, X. Polydimethylsiloxane-Based Superhydrophobic Surfaces on Steel Substrate: Fabrication, Reversibly Extreme Wettability and Oil-Water Separation. *ACS Appl. Mater. Interfaces* **2017**, *9*, 3131-3141.

(68) Guo, F.; Wen, Q.; Peng, Y.; Guo, Z. Simple One-Pot Approach toward Robust and Boiling-Water Resistant Superhydrophobic Cotton Fabric and the Application in Oil/Water Separation. *J. Mater. Chem. A* **2017**, *5*, 21866-21874.

(69) Fu, Q.; Ansari, F.; Zhou, Q.; Berglund, L. A. Wood Nanotechnology for Strong, Mesporous, and Hydrophobic Biocomposites for Selective Separation of Oil/Water Mixtures. *ACS Nano* **2018**, *12*, 2222-2230.

(70) Li, Y.; Zhu, L.; Grishkewich, N.; Tam, K. C.; Yuan, J.; Mao, Z.; Sui, X. CO_2-Responsive Cellulose Nanofibers Aerogels for Switchable Oil-Water Separation. *ACS Appl. Mater. Interfaces* **2019**, *11*, 9367-9373.

(71) Qiu, L.; Sun, Y.; Guo, Z. Designing Novel Superwetting Surfaces for High-Efficiency Oil-Water Separation: Design Principles, Opportunities, Trends and Challenges. *J. Mater. Chem. A* **2020**, *8*, 16831-16853.

For Table of Content

The application of photoredox catalytic amidation for surface functionalization is developed and evaluated. After functionalization with perfluorooctanamide, the filter paper shows excellence water-repellency and hydrophobicity. Besides, it also possesses high wetting selectivity, which can be used to effectively separate the organic/aqueous biphasic mixtures over many cycles without lowering the separating efficiency.

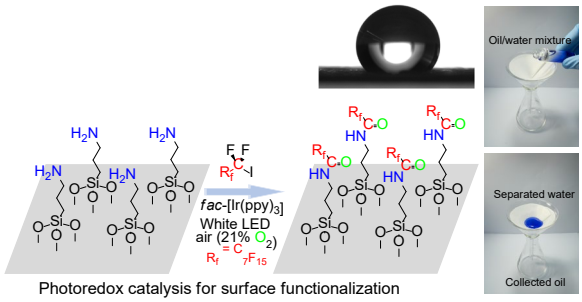

Photoredox catalysis for surface functionalization